

A COMPARISON OF RESULTS FROM NASA'S METEOROID ENGINEERING MODEL TO THE LDEF CRATERING RECORD

S. Ehlert⁽¹⁾, A. Moorhead⁽²⁾, and W.J. Cooke⁽²⁾

⁽¹⁾Qualis Corporation/Jacobs ESSSA Group, Marshall Space Flight Center, Huntsville, AL United States, Email: steven.r.ehlert@nasa.gov

⁽²⁾NASA Meteoroid Environment Office, Marshall Space Flight Center, Huntsville, AL United States

ABSTRACT

NASA's Long Duration Exposure Facility (LDEF) has provided an extensive record of the meteoroid environment in low Earth orbit. LDEF's combination of fixed orientation, large collecting area, and long lifetime imposes constraints on the absolute flux of potentially hazardous meteoroids. The relative impact rate on each of LDEF's fourteen surfaces arises from the underlying velocity distribution and directionality of the meteoroid environment. For the first time, we model the meteoroid environment encountered by LDEF over its operational lifetime using NASA's Meteoroid Engineering Model Release 2 (MEMR2) and compare the model results with the observed craters of potentially hazardous meteoroids (i.e. crater diameters larger than ~ 0.75 mm). We discuss the extent to which the observations and model agree and how the impact rates across all of the LDEF surfaces may be utilized to help calibrate future versions of MEM.

Key words: Meteoroids; Engineering Model; In-Situ Observations.

1. INTRODUCTION

NASA's most complete understanding of the space debris environment is encapsulated in two models. The Orbital Debris Engineering Model [ORDEM, 1] and Meteoroid Engineering Model [MEM, 2] quantify the fluxes of artificial debris particles (hereafter orbital debris) and naturally occurring meteoroids, respectively, expected along a mission's trajectory. These assessments play an essential role in quantifying the total risk to a spacecraft mission during operations. Validating these models against observations is therefore imperative to understanding these risks.

The most recent iteration of MEM [Release 2.05, hereafter MEMR2, 2] was calibrated using a combination of historical data from [3] and more recent observations of meteoroids. While these observations are used to measure the velocity and density distributions of meteoroids,

those properties are intermediate steps in the determination of spacecraft risk. Recent *in-situ* measurements of impact craters on spacecraft offer an independent constraint on the meteoroid cratering rate.

Among all *in-situ* detectors, the spacecraft mission arguably best designed for probing the near-Earth meteoroid flux is the Long Duration Exposure Facility (LDEF). LDEF is a dodecagonal prism that flew in a ~ 480 km altitude, nearly circular orbit around the Earth from April 1984 to January 1990. Its primary mission was to quantify and characterize space environments over its mission lifetime, with the space debris environment constituting one of the top mission priorities. Its attitude was controlled with a gravity gradient to ensure that its two cap surfaces were pointed towards and away from the Earth. Its twelve azimuthal surfaces were maintained to have a fixed orientation relative to its velocity, in essence preserving the directionality of the orbital debris + meteoroid environment within the crater record on each of these twelve surfaces. While most *in-situ* detectors are only sensitive to meteoroids at masses far too small to pose a risk to spacecraft, LDEF had a sufficiently large collecting area and exposure time to detect statistically meaningful samples of impacts from potentially hazardous meteoroids.

In this work we will discuss the extent to which MEMR2 model predicts the observed crater counts on the LDEF spacecraft. This paper is structured as follows: In Section 2 we describe how the output of MEMR2 was utilized to determine the expected number of craters on each surface, while Section 3 provides information about the LDEF crater data utilized in this study. Section 4 shows where the LDEF data are in good agreement or in tension with the MEM prediction, and Section 5 discusses the implications of this investigation for future versions of MEM.

2. THE MODEL

We utilize NASA's MEMR2 to determine the expected flux of sporadic meteoroids each surface of LDEF. The

state vectors of LDEF were sampled at 910 minute intervals from the spacecraft’s two-line element (TLE) files. Given the 94 minute orbital period of LDEF, this sampling corresponds to once every 9.68 orbits. Because the meteoroid environment depends strongly on the relative location of the spacecraft but is largely independent of time, an accurate meteoroid flux estimate requires sampling at every state vector along the spacecraft’s orbit but not sampling the same position on every individual orbit. The choice of sampling every 9.68 orbits enables an accurate meteoroid flux to be calculated without performing redundant calculations.

We used a mass limit of 10^{-6} g, the minimum value allowed by MEM. Meteoroids smaller than 10^{-6} g are subject to different forces during their orbits and likely have a significantly different velocity distribution than that assumed for the higher mass meteoroids that are the focus of MEM. We sample velocities that range from $0 - 72 \text{ km s}^{-1}$ relative to the spacecraft. MEMR2 assumes a single density of 1 g cm^{-3} for all meteoroids. We calculated the velocity and direction dependent flux using the finest available binning: velocity bin sizes were set to 2 km s^{-1} and angular bin sizes were set to $1^\circ \times 1^\circ$.

2.1. Crater Model

The LDEF data constitutes a crater-diameter-limited sample whereas the initial output of MEM is a mass-limited sample. Because the expected diameter of a crater depends on both the mass and velocity of the impactor, the mass-limited fluxes calculated by MEM were converted into a crater-diameter-limited fluxes for each velocity bin using the Cour-Palais cratering equation of [4] and the material properties listed in [5]. The mass of a particle (m , in g) was related to a given crater diameter (d , in cm), its velocity normal to the spacecraft surface (v_\perp), and density (ρ_m) as

$$m = \frac{\pi}{6} \left(\frac{0.527d}{5.24} BH^{0.25} \rho_m^{-4/27} \left(\frac{v_\perp}{c_t} \right)^{-2/3} \rho_t^{1/2} \right)^{54/19} \quad (1)$$

where BH corresponds to Brinell Hardness of the target, ρ_m corresponds to the density of the meteoroid (1 g cm^{-3} for MEM), c_t is the speed of sound of the target material, and ρ_t is the density of the target material. The leading factor of 0.527 converts the crater diameter as measured by LDEF into the crater depth into the target material as discussed in [5, and references therein]. All of the impacts penetrated targets composed of 6061-T6 aluminum alloy. This particular alloy has a Brinell Hardness of $BH = 90$, a sound speed of $c_t = 6.1 \text{ km s}^{-1}$, and a density of 2.70 g cm^{-3} .

Since the MEMR2 output provides the mass-limited flux of meteoroids at individual velocities, we adjust the mass-limited fluxes for each velocity bin into a crater-diameter-limited flux. Using the limiting mass calculated for a given velocity, limiting crater diameter, and impact direction we re-weight the initial mass-limited flux calculated

by MEMR2 to new limiting masses using the mass distribution of [3]. It is critical to emphasize that MEMR2’s direction-dependent output is crucial for this comparison, since the incidence angle between the velocity vector and the surface normal vector influences both the incident flux of meteoroids onto the surface in question and the size of craters produced by meteoroids of a given mass.

3. THE DATA

As stated above, the fourteen surfaces of LDEF were at fixed orientations relative to the spacecraft’s velocity during its orbit. In the standard LDEF labeling scheme, the ram direction was offset 8 degrees from the normal of Surface #9, in the direction of Surface #10. Surface # 12 was just offset from North, and Surface #6 was just offset from South. Surfaces #13 and #14 correspond to the space-facing and Earth-facing surfaces of LDEF, respectively.

Since orbital debris particles are nearly always in bound, circular orbits around the Earth whereas meteors are nearly always in unbound orbits, all impacts on the space-facing surface are assumed to originate from meteoroids. Because of shielding by the Earth, all impacts on the Earth-facing surface must occur at extreme angles, and we do not utilize the impact record on this surface in this work. The twelve azimuthal surfaces are assumed to arise from the sum of the orbital debris and meteoroid environments. The orientation of the azimuthal surfaces relative to its velocity is shown in Figure 1.

The Chemistry of Micrometeoroids Experiment (CME) was an additional set of test surfaces on LDEF which investigated the chemical properties of residue around impact craters on sides #3 (wake) and #11 (52° north of ram) using gold and aluminum targets, respectively. The gold target on Surface # 3 and the aluminum target on Surface #11 are identified with gold and silver rectangles in Figure 1, respectively.

3.1. The Crater Record

The primary LDEF data set against which we compare MEM is the crater record from the Space Debris Impact Experiment [6]. These data constitute a search for craters with lip diameters greater than $1000 \mu\text{m}$ across the surfaces of the Space Debris Impact Experiment on each of LDEF’s fourteen faces. The investigated area and number of craters found on each of the fourteen surfaces can be found in Table 1. As discussed in this same paper, the limiting crater lip diameter of $1000 \mu\text{m}$ corresponds to a limiting crater diameter of $d = 750 \mu\text{m}$ for use in Equation 1.

This limiting crater diameter of $750 \mu\text{m}$ corresponds to mass of 10^{-6} g (the minimum mass limit of MEMR2) for a meteoroid with a velocity of $\sim 47 \text{ km s}^{-1}$. Since the

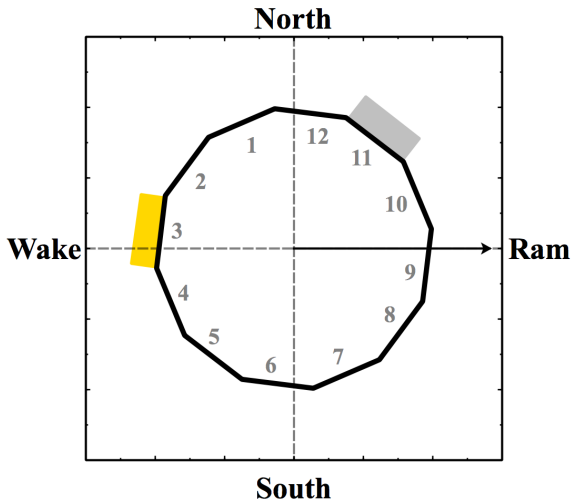


Figure 1. The exposure geometry of LDEF visualized. The standard LDEF side numbers are labelled along with the ram, wake, north, and south directions. The gold rectangle indicates that the gold target of the Chemistry of Micrometeoroids Experiment (CME) was located on Surface # 3, while the silver rectangle corresponds to the location of the aluminum target of the CME on Surface # 11.

crater diameter increases with increasing velocity, meteoroids with relative speeds (normal to the spacecraft surface) greater than 47 km s^{-1} have a corresponding limiting mass less than 10^{-6} g . As a result, the re-scaled fluxes we have calculated constitute a strict underestimate of the total flux of meteoroids that may produce the observed craters. The relative fraction of the meteoroid population that is unaccounted for by our MEMR2 calculations due to this sampling bias cannot be reliably estimated since the dynamics of these low mass meteoroids are dominated by forces not accounted for in MEMR2. However, based on similar calculations at larger limiting crater diameters where the MEMR2 mass limit is not reached we expect the relative flux ratios between each of the surfaces to be unaffected by this sampling bias.

We have also investigated the intercostal crater record discussed in [7]. These data have three limitations relative to the data set presented in [6], however, in the context of this study. First, the collecting area is significantly smaller on each surface, which results in smaller sample sizes and larger statistical uncertainties. Secondly, the limiting crater diameter of the intercostal data is smaller ($640 \mu\text{m}$ as compared to $750 \mu\text{m}$ for [6]), which exacerbates the systematic uncertainty associated with measuring the flux of meteoroids that lies partially below MEMR2's mass limit. Finally, the intercostal crater data set is limited to the twelve azimuthal surface of the spacecraft: no measurements of the cratering record on the space facing surface are available. For these reasons, we omit the results of a comparison between MEMR2 and

Table 1. The crater record from the Space Debris Impact Experiment aboard LDEF as published in [6]. The limiting crater lip diameter for these data is $d_{\text{lip}} > 1000 \mu\text{m}$.

Surface	Label	Craters	Area (m^2)
1		2	3.84
2		1	2.26
3	Wake	3	1.48
4		2	2.66
5		3	2.66
6	South	9	3.26
7		17	3.69
8		8	1.08
9	Ram	14	0.913
10		22	1.48
11		21	3.84
12	North	8	1.33
13	Space	17	5.48
14	Earth	1	8.16

the intercostal data here.

3.2. Disentangling Orbital Debris from Meteoroids

Because LDEF was subject to impacts from both orbital debris and meteoroids during its mission, any comparison between MEM and LDEF cratering record requires an estimate of the relative impact rates of these two populations on each surface. Our estimate is derived from the published results of the CME, the details of which can be found in [8]. They argue that orbital debris constitutes 10% of the impacts on the wake facing surface (side #3, equipped with a gold target) and 45% of the impacts on the forward facing surface (side #11, equipped with an aluminum target). As stated above, we assume that the space-facing side is free of orbital debris impacts. Because of the large model uncertainties on the orbital debris environment during the LDEF mission, no attempts at modeling the orbital debris contribution to the flux on the other ten surfaces have been made.

4. COMPARING THE MODEL AND THE DATA

4.1. The Space Facing Side of LDEF

Because the space facing side of LDEF should be subject to virtually no impacts from orbital debris, we can compare the data and MEM predictions for LDEF directly. MEM predicts a total of 11.40 craters with $d > 750 \mu\text{m}$ on the space facing plates over the duration of the LDEF mission. A total of 17 craters were identified in this surface [6], suggesting an absolute deviation between the data and the model of $\sim 50\%$. The cumulative distribution function of a Poisson distributed variable with a mean of $\mu = 11.40$ indicates that there is a $\sim 4\%$ chance

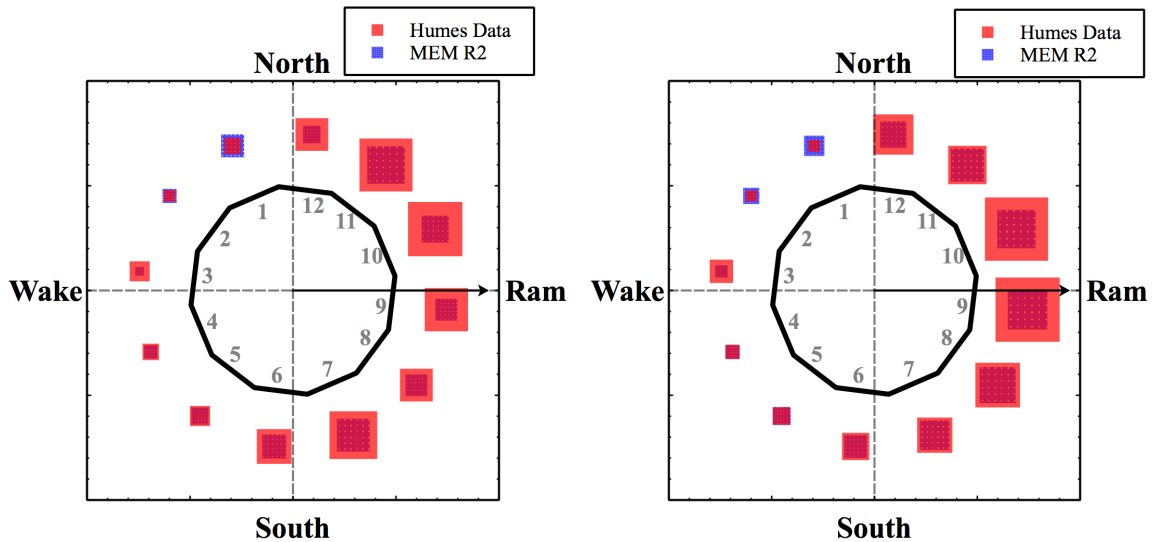


Figure 2. A comparison between the number of observed and modeled crater fluxes on the twelve azimuthal surfaces of LDEF before accounting for orbital debris. In both figures, the areas of the red and blue squares are proportional to the observed and predicted number of craters on each surface, respectively. The left sub-figure shows the absolute crater counts on each surface, while the right sub-figure shows the flux ratio on each surface relative to the space-facing surface.

of observing 17 or more craters. The observed LDEF craters on this surface could therefore be interpreted as a rare but nevertheless plausible realization of MEMR2.

4.2. The Azimuthal Sides

We investigate MEMR2’s predictions of the craters on each of the twelve azimuthal surfaces in two ways. We first compare the number of craters observed on each surface with the number predicted by MEMR2. We perform a second comparison between the observed and predicted craters calculating the ratio between each azimuthal surface flux and the flux on the space-facing surface. Both of these comparisons are subjected to systematic uncertainties associated with orbital debris contamination. We therefore include for each of our two model/data comparisons two model variants: one that includes only meteoroids (i.e. the output of MEM alone) and one that accounts for craters originating from orbital debris using our estimate of the orbital debris fraction on surfaces #3 and #11.

4.2.1. Crater Counts

The number of craters expected and observed for each of the twelve azimuthal surfaces (as well as the space-facing surface) can be found in Table 2 and illustrated in the left panel of Figure 2.

The largest discrepancy is seen on Surface # 1, where significantly more craters were predicted by MEMR2 than

Table 2. The crater counts on each azimuthal surface of LDEF as compared to MEM predictions. The first column presents the total number of craters observed on each surface, while the second and third columns separate the observed crater counts into expected meteoroid and orbital debris counts based on the relative contribution of orbital debris on that same surface. Surfaces # 3, #11, and #13 (the wake, ram, and space-facing surfaces) are the only three for which estimates of the orbital debris fraction can be estimated from previous studies. No chemical analysis is available for the craters presented here, and we therefore cannot associate individual craters with meteoroids or orbital debris in this data set. The fourth column shows the number of meteoroid craters predicted by MEMR2.

Surface	Observed	OD	Meteoroids	MEM
1	2	–	–	3.95
2	1	–	–	1.61
3 (Wake)	3	0.3	2.7	0.91
4	2	–	–	1.71
5	3	–	–	2.20
6 (South)	9	–	–	4.25
7	17	–	–	8.03
8	8	–	–	3.5
9 (ram)	14	–	–	3.56
10	22	–	–	5.42
11	21	9.45	11.55	10.46
12 (North)	8	–	–	2.27
13 (Space)	17	0	17	11.40

observed. This over-prediction is independent of any estimate for the orbital debris contribution. On Surface #3, where the orbital debris fraction was estimated at $\sim 10\%$, MEMR2 slightly under-predicted the total number crater counts (3 total craters/2.7 meteoroid craters observed versus 0.91 meteoroid craters predicted). On Surface #11, where the orbital debris fraction has been estimated to be $\sim 45\%$, MEMR2 predicts 10.46 craters from meteoroid impacts. This prediction is fully consistent with the 21 total craters and 11.55 meteoroid craters observed on this surface. For Surfaces # 9 and #10 on the ram-facing side, MEMR2 appears to predict significantly fewer craters than what were observed, a tension that persists even when assuming the same orbital debris contribution of Surface # 11 (45%). In order to reconcile the MEMR2 prediction with the observed crater counts, an orbital debris contribution of $\sim 75\%$ is required for these two surfaces.

4.2.2. Flux Ratios to the Space Facing Side

The calculated ratios of the azimuthal surface-specific flux to the flux on the space-facing surface are shown in Table 3 and illustrated in the right panel of Figure 2. For each surface we present the expected and observed flux ratios. We have also determined the asymmetric 68% confidence interval on the observed flux ratios assuming Poisson fluctuations for the observed number of craters on each surface. Due to the large statistical uncertainties expected for each observation, the majority of the surface flux ratios are consistent between the MEMR2 prediction and the observed crater counts. However, several surfaces show tension between the observations and their corresponding MEMR2 predictions. The tension is most clearly observed on Surface #1, where MEMR2 predicts a significantly higher flux ratio than what was observed. The predicted flux ratio for Surface #3 was lower than what was observed, although with only three observed craters on this surface the MEMR2 prediction is formally consistent with the observations. For the one ram-facing surface where the orbital debris contribution can be estimated (Surface #11), the observations are fully consistent with the MEMR2 prediction. The other ram-facing surfaces generally have observed flux ratios that are significantly higher than the MEMR2 prediction. If we assume the same orbital debris contribution for these surfaces as we assumed for Surface #11 this tension still persists. The discrepancy is especially pronounced for Surfaces #9 and #10 that are closest to the ram direction. Without a model estimate of the orbital debris contribution to the fluxes on these surfaces, however, we cannot quantify the significance of this tension.

5. DISCUSSION

This investigation demonstrates that the MEMR2 meteoroid environment is generally in good agreement with the cratering record of LDEF. Since the ultimate goal of

MEMR2 is to provide an accurate assessment of the risk the meteoroid environment poses to spacecraft, our results support the use of NASA's Meteoroid Engineering Model in mission planning and risk assessment. Absolute deviations in the predicted versus observed number of craters with diameters of $d > 750 \mu\text{m}$ in general agree to within $\sim 50\%$. The relative fluxes observed between the twelve azimuthal surfaces of LDEF and the space-facing surface are also generally in good statistical agreement with the MEMR2 predictions.

Although the LDEF cratering record and the predicted flux as calculated by MEMR2 are generally in good agreement, there is nevertheless evidence of tension between the model and observations on individual surfaces. The most statistically significant discrepancies occur on Surface #1 in the north-wake quadrant, where MEM over-predicts the number of craters on this surface by a factor of ~ 2 . The number of craters on the ram-facing Surfaces #9 and #10 appear to be under-predicted by MEMR2, although this discrepancy could in principle be reconciled by an orbital debris contribution of $\sim 75\%$ for these two surfaces. For the three surfaces where the orbital debris fraction can be constrained by observational data, MEMR2 accurately predicts the total number of craters on one of the surfaces (#11) and under-predicts the total number of craters on the other two (#3 and the space-facing surface).

A more thorough investigation into the orbital debris contribution on the sides other than the three discussed in detail here requires a model of the orbital debris environment during LDEF's mission lifetime (1984 – 1990). Observational constraints on the orbital debris environment from this time window are sparse, and modern orbital debris models cannot be reliably extrapolated backwards to this time. It is beyond the scope of this work to develop an orbital debris environment model for this mission.

There are several additional caveats with regards to this comparative study that may indicate a larger but unpredictable discrepancy between MEMR2 and the crater record. Most significantly, the crater data we utilized are subject to a sampling bias with respect to MEMR2's mass limit. Our re-scaled MEMR2 predictions are therefore strict underestimates for every surface by an uncertain factor. The particular value of this bias factor is not straightforward to estimate, but appears to be constant across all of the LDEF surfaces. We also emphasize that the accuracy of any comparison of this nature is limited by the accuracy of the assumed crater model/ballistic limit equation and target material properties. Assuming the aluminum material properties of [4] rather than those [5], for example, can increase the predicted number of craters on LDEF by $\sim 20 - 25\%$. We therefore expect systematic uncertainties in our prediction to arise from our particular choice of a ballistic limit equation.

These LDEF data also offer an opportunity to provide an independent constraint on the meteoroid velocity distribution in the manner described by [9]. Using the analytic

Table 3. The ratio of fluxes on each azimuthal surface of LDEF to the space-facing side along with the MEM predictions for the same flux ratio. The first column presents the flux ratio using all craters relative to the space-facing surface, whereas the second column provides the same ratio for the meteoroid craters after correcting for the estimated contribution of orbital debris. Surfaces # 3, #11, and #13 (the wake, ram, and space-facing surfaces) are the only three for which estimates of the orbital debris fraction can be estimated from [8]. No chemical analysis is available for the craters presented here, and we therefore cannot associate individual craters with meteoroids or orbital debris in this data set. The final column provides the predicted flux ratio from MEMR2.

Surface	Observed	Observed (OD corrected)	MEM
1	$0.159^{+0.147}_{-0.094}$	–	0.49
2	$0.135^{+0.168}_{-0.135}$	–	0.34
3 (Wake)	$0.617^{+0.472}_{-0.370}$	$0.555^{+0.454}_{-0.338}$	0.30
4	$0.229^{+0.213}_{-0.139}$	–	0.31
5	$0.343^{+0.275}_{-0.206}$	–	0.40
6 (South)	$0.890^{+0.455}_{-0.330}$	–	0.63
7	$1.485^{+0.619}_{-0.437}$	–	1.05
8	$2.368^{+1.214}_{-0.918}$	–	1.56
9 (Ram)	$4.911^{+2.092}_{-1.481}$	–	1.87
10	$4.792^{+1.873}_{-1.284}$	–	1.76
11	$1.763^{+0.684}_{-0.494}$	$0.951^{+0.476}_{-0.309}$	1.31
12 (North)	$1.923^{+0.961}_{-0.711}$	–	0.82

framework described in this paper, variations between the surface crater counts provide a direct measure of the velocity distribution if the integrated meteoroid environment for LDEF is assumed to be isotropic before accounting for the spacecraft's motion¹. To confirm that MEMR2 is consistent with this assumption, we have run MEMR2 using a modified set of LDEF state vectors. This second set has identical positions and times, but every velocity component was divided by a factor of 1000 to minimize any influences arising from the spacecraft's velocity. The resultant flux maps are consistent with an isotropic distribution, suggesting that the relative crater counts on each surface can in fact be used in this manner. This methodology is ideally suited for testing an assumed velocity distribution's consistency with the LDEF cratering record.

We have developed a framework to compare future versions of MEM with the LDEF cratering record. Any changes in MEM's directionality, speed distribution, or meteoroid bulk density will ultimately change the predicted crater counts on each spacecraft surface. Validating environment models against *in-situ* crater data such as LDEF helps ensure an accurate assessment of the risk meteoroid impacts pose to future spacecraft missions. Even without orbital debris estimates for ten of the thirteen surfaces utilized here, the LDEF crater record can be used to constrain meteoroid environment models such as MEM.

ACKNOWLEDGMENTS

This work was supported by NASA's Meteoroid Environment Office under NASA Contract MSFC-NNM12AA41C (SE). We thank Dr. Robert Suggs for many conversations that have helped improve the figures and text of this paper.

REFERENCES

1. E. Stansbery, M. Matney, P. Krisko, P. Anz-Meador, M. Horstman, J. Opiela, E. Hillary, N Hill, R. Keley, A. Vavrin, and D. Jarkey. NASA Orbital Debris Engineering Model (ORDEM) 3.0 - User's Guide. Technical Report NASA/TP-2014-217370, NASA Johnson Space Center, April 2014.
2. A.V. Moorhead, H.M. Koehler, and W.J. Cooke. NASA Meteoroid Engineering Model (MEM) Release 2.0. Technical Report NASA/TM-2015-218214, NASA Marshall Space Flight Center, October 2015.
3. E. Grün, H. A. Zook, H. Fechtig, and R. H. Giese. Collisional Balance of the Meteoritic Complex. *Icarus*, 62:244–272, May 1985.
4. K.B. Hayashida and J.H. Robinson. Single Wall Penetration Equations. Technical Report NASA/TM-103565, NASA Marshall Space Flight Center, December 1991.
5. S. G. Love and D. E. Brownlee. A Direct Measurement of the Terrestrial Mass Accretion Rate of Cosmic Dust. *Science*, 262:550–553, 1995.
6. D. H. Humes. Small Craters on the Meteoroid and Space Debris Impact Experiment. In *LDEF: 69 Months in Space. Third Post-Retrieval Symposium*, February 1995.
7. M. Zolensky, D. Atkinson, T. See, M. Allbrooks, C. Simon, and M. Fincknor. Meteoroid and Orbital Debris Record of the Long Duration Exposure Facility's Frame. *Journal of Spacecraft and Rockets*, 28(2):204–209, 2016/11/08 1991.
8. F. Hörz, T. H. See, R. P. Bernhard, and D. E. Brownlee. Natural and Orbital Debris Particles on LDEF's Trailing and Forward-Facing Surfaces. In *LDEF: 69 Months in Space. Third Post-Retrieval Symposium*, February 1995.
9. H. A. Zook. Deriving the Velocity Distribution of Meteoroids from the Measured Meteoroid Impact Directionality on the Various LDEF Surfaces. In A. S. Levine, editor, *LDEF, 69 Months in Space : First post-retrieval symposium*, volume 3134 of *NASA Conference Publication*, page 569, 1991.

¹This model discussed in [9] explicitly accounts for shielding by the Earth.